Bimoment loads on space frame elements

Maicon José Hillesheim[1], Francisco Célio de Araújo[2]

[1]*Faculdade de Ciências exatas e Tecnológicas do Campus de Sinop, Universidade do Estado de Mato Grosso*
Avenida dos Ingás 3001, 78555-000, Sinop/Mato Grosso, Brazil
jose.maicon@unemat.br
[2]*Dept. de Engenharia Civil, Universidade Federal de Ouro Preto*
Rua Nove, 293, 35400-000, Ouro Preto/Minas Gerais, Brazil
dearaujofc@gmail.com

Abstract. This paper presents an algorithm based on the Direct Stiffness Method to solve bars with composite variable cross sections under nonuniform torsion. In this formulation, the primary and secondary torsion modes are described by 2D Neumann's boundary-value problems, which are solved at the cross-section level by employing the BEM. The torsional rotation angle along the element length is described by a set of ordinary differential equations, which are solved by using weighted residual techniques. Herein, a *n*th-order polynomial is adopted to approximate the torsion angle function. In this paper, we will especially assess the effects of external bimoment loads on the calculation of stresses along the beam. Accuracy of the formulation is observed by comparing results obtained with the present beam formulation and 3D solid ANSYS models.

Keywords: Nonuniform torsion, composite bars with variable cross sections, the BEM, torsion-related element stiffness matrices.

1 Introduction

Bar structural elements subjected to nonuniform torsion are often found in space frames, such as in curved elements of viaducts, in shafts of machine elements, etc, which may also have composite cross sections with variable stiffness. Several works available in the literature, such as [1],[2],[3], have applied the Boundary Element Method to obtain the corresponding warping functions and to include secondary torsion moment deformation effect (STMDE) in the analysis, providing very satisfactory results for this class of problem in practical situations. However, the numerical examples presented in these studies not always show the clear effect of torsional moment loads on the final normal stress distributions in the cross sections of the element. In this context, the present article aims to demonstrate that an axial load applied at a given point of the cross section generates, in addition to the well-known bending effects, nonuniform torsion effects and a corresponding increase in normal stresses, which correct the classical beam theories. Accuracy of the formulation is assessed by comparing results obtained with the present beam formulation and 3D solid ANSYS models.

2 Statement of the problem

When an eccentric axial load is applied to a beam, in addition to the known asymmetric bending (bending moment in two directions and normal stress), a localized bimoment load is applied to the beam, which induces non-uniform torsion. Figure 1- (a) shows a bar referenced in the x,y,z system with an axial load applied as mentioned above, at the free end. In Figure 01-b, the deformed aspect of the bar is shown.

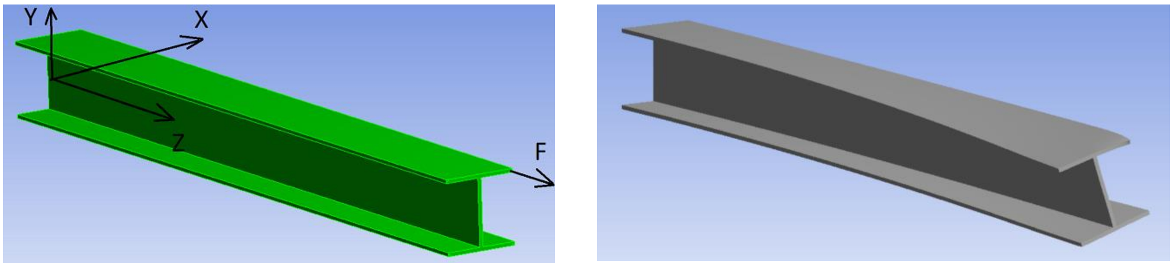

(a)Bar element with eccentric load. (b)Aspect of the deformed bar.

Figure 1. Bar subjected to an eccentric axial force.

According to the classical Euler−Bernoulli beam theory, the load can be reduced to an axial force applied at the geometric center of the cross section and two local moment components, $M_x^e = F \cdot e_y$ and $M_y^e = F \cdot e_x$. Taking a cross section located at any position z, but not too close to the free end, the stress component σ_z is given by Eq. 1.,

$$\sigma_z = \frac{M_x(z)}{I_x} y - \frac{M_y(z)}{I_y} x + \frac{N(z)}{A}, \tag{1}$$

where, I_x is the moment of inertia about the x-axis, I_y is the moment of inertia about the y-axis, A is the cross-sectional area, and M_x(z), M_y(z), and N(z) are the internal forces at the cross sections.

However, when observing the deformed aspect of the bar in Figures 1-(b), bending in relation to the x axis and the y axis, and rotation in relation to the longitudinal axis will be observed. Another notable aspect is the warping of the cross section. This is due to the fact that the applied load, as mentioned, also corresponds to the application of bimoment load at the free end, causing nonuniform torsion in addition to asymmetric bending. The intensity of the respective bimoment is equivalent to the product of the force and the warping function, $\psi^p(\boldsymbol{x})$, of the cross section at the point of application of the force. It is worth noting that the warping functions an intrinsic property of the cross section.

In general, a cross section located at any z coordinate is subjected, in addition to bending moments and normal force, to a bimoment, and to primary and secondary torsional moments. To find the value of these section moments, one has to solve the nonuniform torsion problem.

Just as a point load produces local moments and bimoments, a distributed axial load applied outside the geometric center of the cross section generates distributed bimoment, $m_\psi(z)$, as illustrated in Figure 2-(a). Transverse loads can generate torque loads as illustrated in Figure 2-(b).

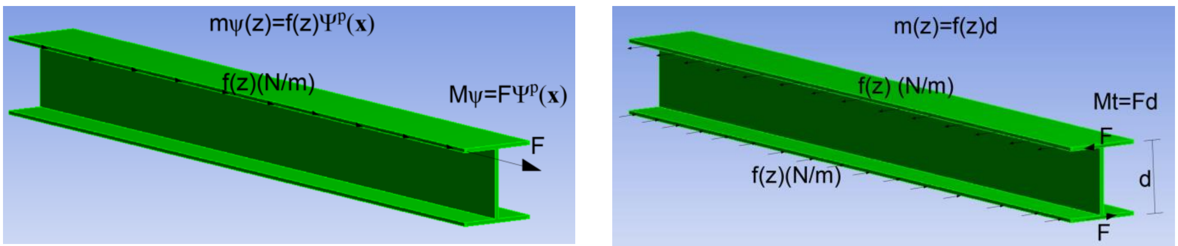

(a)Loads that generate bimoments. (b) Loads that generate twist moments.

Figure 2. Generalization of externally applied moments.

To understand the nonuniform torsion, consider Figure 03. The double arrows denote a distributed torsional moment load $m(z)$, and the triple headed arrows represent an external bimoment load, $m_\psi(z)$.

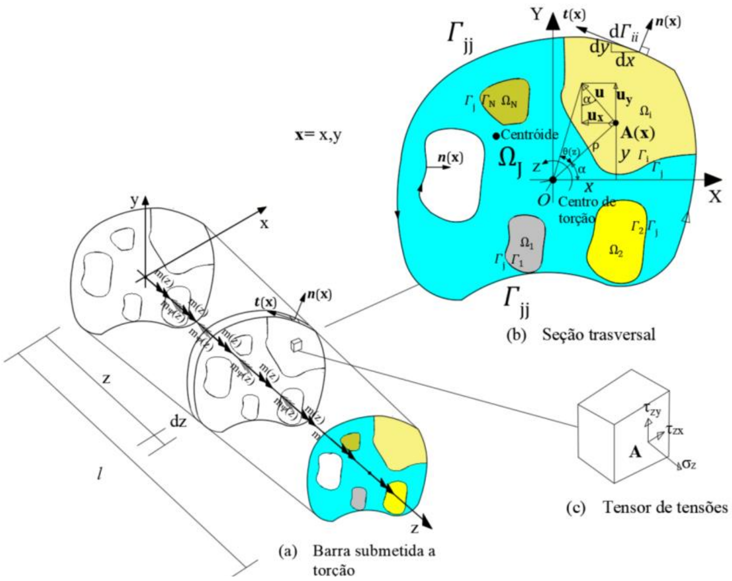

Figure 3. Composite beam under nonuniform torsion.

In the context of nonuniform torsion, considering the SMTD, the angular displacement field is separated into two components, the primary and secondary ones. Thus, we have (see Eq. 2),

$$\theta(z) = \theta^p(z) + \theta^s(z). \tag{2}$$

From the plane geometry, observing the cross section illustrated in Figure 3-(b), it is possible to demonstrate that the respective angular displacement field is related to the Cartesian displacement field of point A, through the expressions given in Equations 3,

$$\begin{aligned} u_x &= -(\theta^p + \theta^s)y, \\ u_y &= (\theta^p + \theta^s)x, \\ u_z &= \frac{d\theta^p}{dz}\psi^p(\boldsymbol{x}) + \frac{d\theta^s}{dz}\psi^s(\boldsymbol{x}). \end{aligned} \tag{3}$$

Taking then the displacement field into the stress and strain relations of the theory of elasticity, it is verified that the normal stress component due to non-uniform torsion is given by Eq. 4,

$$\sigma_z =\cong E_i \frac{d^2\theta^p}{dz^2}\psi^p, \tag{4}$$

and the shear stresses components according to Equations 5,

$$\begin{aligned} \tau_{xz} &= G_i \frac{d\theta}{dz}\left(\frac{\partial\psi^p}{\partial x} - y\right) + G_i \frac{d\theta^s}{dz}\left(\frac{\partial\Delta\psi}{\partial x}\right), \\ \tau_{yz} &= G_i \frac{d\theta}{dz}\left(\frac{\partial\psi^p}{\partial y} + x\right) + G_i \frac{d\theta^s}{dz}\left(\frac{\partial\Delta\psi}{\partial y}\right), \end{aligned} \tag{5}$$

where E_i and G_i correspond to the transverse longitudinal modulus of elasticity of the i-th material present in the cross section respectively, $\frac{d\theta}{dz}$ is the angular displacement rate, $\frac{d\theta^s}{dz}$ is the secondary angular displacement rate and $\frac{d^2\theta^p}{dz^2}$ is torsional curvature of the primary portion of the angular displacement.

Replacing the stresses in the equilibrium equations of the elasticity, the boundary value problems that describe the warping functions are obtained. The first warping mode is described by the Laplace’s partial differential equation, and the higher modes are governed by Poisson’s partial differential equation. The resolution of these boundary value problems is carried outby applying the Boundary Element Method, in which details can be seen in [3].

Considering a segment of infinitesimal length dz of a bar subjected to the efforts indicated in Figure 4, performing the balance of forces, the global ordinary differential equations are obtained: Eq. 6 for the equilibrium of torsional moments, and Eq. 7 for the equilibrium of bimoments. For both Equations, the independent variables are the components of the angle of twist. The boundary conditions of Equations 6 and 7 are given by Equations 8 and 9.

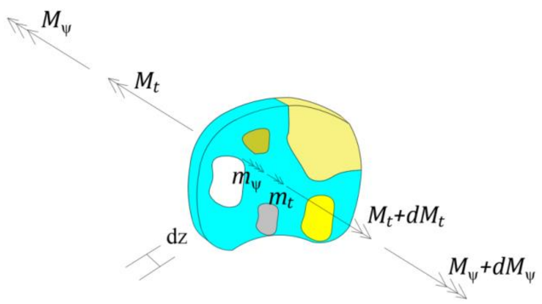

Figure 4. Segment of length dz.

$$\sum M_t = \frac{dM_t}{dz} + m(z) = \frac{d}{dz}\left[k_t^p(z)\frac{d\theta(z)}{dz} + k_t^s(z)\frac{d\theta^s(z)}{dz}\right] + m(z) = 0 \tag{6}$$

$$\sum \frac{dM_\psi}{dz} = M_t^s(z) + m\psi(z) = \frac{d}{dz}k_\psi(z)\cdot\frac{d^2}{dz^2}\theta^p(z) + k_\psi(z)\cdot\frac{d^3}{dz^3}\theta^p(z) + m\psi(z) = 0. \tag{7}$$

Note that to solve a bar subjected to nonuniform torsion, considering an external bimoment load, it is enough to impose this load as a boundary condition in Eq. 9. Furthermore, Equations 8 and 9 allow the imposition of the most general possible boundary conditions.

$$\alpha_1(z)\theta(z) + \alpha_2(z)M_t(z) = \alpha_3 \tag{8}$$

$$\beta_1(z)\frac{d\theta^p(z)}{dz} + \beta_2(z)M_\psi(z) = \beta_3 \tag{9}$$

For Equations 6, 7, 8 and 9, the bimoment along the bar is given according to Eq. 10 and is related to the primary angular displacement.

$$M_\psi = -\sum_{i=1}^{nsub} E_i \int [\psi^p(\boldsymbol{x})]^2 d\Omega_i \cdot \frac{d^2\theta^p(z)}{dz^2} = -k_\psi(z)\frac{d^2\theta^p(z)}{dz^2} \tag{10}$$

The torque is the resultant of the shear stresses, that is, $M_t = \sum_{i=1}^{nsub} \int \left(x\tau_{zy} - y\tau_{zx}\right) d\Omega_i$, knowing the shear stresses were separated into two parts, the primary torsional moment is given by Eq. 11,

$$M_t^p = \sum_{i=1}^{nsub} G_i I_{ti}^p \frac{d\theta}{dz} = k_t^p \frac{d\theta}{dz}. \tag{11}$$

and the secondary torsional moment along the bar is given according to Eq. 12,

$$M_t^S = \sum_{i=1}^{nsub} G_i I_{ti}^S \frac{d\theta^s}{dz} = k_t^S \frac{d\theta^s}{dz}. \tag{12}$$

For Equations 6, 7, 8, 9, 10, 11 and 12, the warping stiffness k_ψ, the primary torsional stiffness k_t^p and the secondary torsional stiffness k_t^s, are given in Equations 13, 14 and 15 respectively,

$$k_\psi(z) = \sum_{i=1}^{nsub} E_i \int [\psi^p(\boldsymbol{x})]^2 d\Omega_i\,(z), \tag{13}$$

$$k_t^p = \sum_{i=1}^{nsub} G_i \left[\iint x\left(\frac{\partial\psi^p}{\partial y} + x\right) - y\left(\frac{\partial\psi^p}{\partial x} - y\right) d\Omega_i\right], \tag{14}$$

$$k_t^s = \frac{\left(k_\psi\right)^2}{\left(\sum_{i=1}^{nsub} G_i \int \boldsymbol{\nabla}\Delta\bar{\psi} \cdot \boldsymbol{\nabla}\Delta\bar{\psi} d\Omega_i\right)}. \tag{15}$$

To solve the ordinary differential equations, Equations 6 and 7, the angular displacements are approximated by polynomials, and their parameters obtained through the method of the weighted residuals method, according to Equations 16 and 17,

$$\int_0^l \{\mathcal{L}_1[\theta^p(z), \theta^s(z)] + m(z)w_k\}\, dz = 0, \tag{16}$$

$$\int_0^l \left\{\mathcal{L}_2[\theta^p(z), \theta^s(z)] + m_\psi(z)w_k\right\} dz = 0, \tag{17}$$

where the weighting function is defined by Eq. 18,

$$w_k = z^{k=0} \cdots z^{k=d-4} \tag{18}$$

Applying the weighted residual method results in a system of algebraic equations whose unknown variables are the coefficients of the torsion angle polynomials. Note that the distributed torsional moment and distributed bimoment load will appear on the right-hand side of the system of equations.

Once the components of the angular displacement as well as their derivatives are known, the stresses along the bar may be obtained as well as the bimoment, primary and secondary torsion moments. Thus, the normal stress along the bar ─ with the additional inclusion of nonuniform effects ─ will be given by Eq. 19 (c.f. Eq. 01) below. Shear stresses are calculated according to Equations 5.

$$\sigma_z = \frac{M_x(z)}{I_x} y - \frac{M_y(z)}{I_y} x + \frac{N(z)}{A} - \frac{M_\psi(z)}{C_\psi(z)} \psi^p(\boldsymbol{x}, z) \tag{19}$$

3 Numerical example

Let us consider the steel bar with E=200GPa and G=76.923GPa. The dimensions are shown in Figures 5-(a) and Figure 5-(b), the mesh of boundary elements in Figure 5-(c). The bar is clamped at the end z = 0, and has a tensile load of 1.0 x10^5N applied to the upper right corner, where the warping function is 0.036 m, resulting in a bimoment M_ψ=3700Nm^2, M_x^e =20kNm, $M_y^e = -20$kNm, N=100kN. Initially, the effects of nonuniform torsion are solved with beam theory, in which the stiffnesses defined in Equations 13, 14 and 15 are obtained with the boundary elements algorithm and their values, shown in table 1.

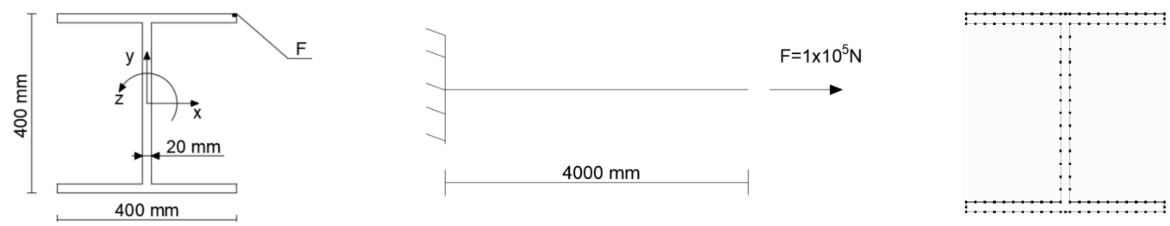

(a). Cross section. (b)Longitudinal representation. (c). BE mesh

Figure 5Details of the analyzed structure.

Table 1 - Cross section properties

k_t^p (Nm^2)	k_t^s (Nm^2)	k_ψ (Nm^4)
235342.05	37568755.66	1535486.85

With these properties, differential Equations 6 and 7 are solved, in which the following boundary conditions are considered: for z = 0, we have $\alpha_1 = 1$, $\alpha_2 = 0$, $\beta_1 = 1$, $\beta_2 = 0$ e $\beta_3 = 0$. For z=4m, we have $\alpha_1 = 0$, $\alpha_2 = 1$, $\alpha_3 = 0$, $\beta_1 = 0$, $\beta_2 = 1$ e $\beta_3 = 3700$.

The weighted residuals method is then applied, and the differential equations 5 and 6 have been solved, and the angle of twist is obtained. Knowing the portions of the angular displacement, the distribution of internal forces is calculated according to Equations 10, 11 and 12, and then presented in Figure 6-(b). To validate the proposed theory, the displacement obtained with the present study is compared with the refined 3D solid analysis obtained with the ANSYS package. To convert the 3D solid analysis results, the displacements $u_x(z)$ along the length of the beam at the top of the cross sections of beam are measured, subtracted from the portion of displacements coming from the bending measured at the geometric center of the cross section and then divided by the distance from the top line to the center of twist according to equations 3. The comparison of results is shown in Figure 6 (a).

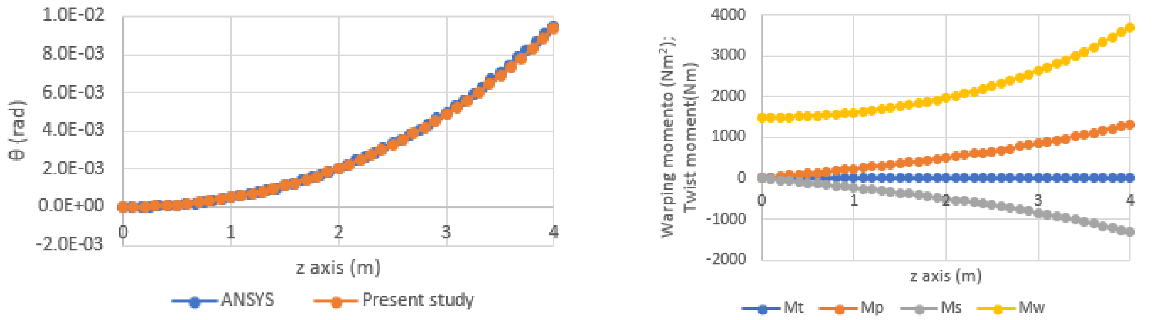

(a). Angle of twist (b). Intenal forces

Figure 6. Quantities of interest.

In a section located at coordinate z =1.0m, the normal stresses due to bimoment and shown in Figure 7-(a) and the stresses due to asymmetric bending, shown in Figure 7-(b) are evaluated. In Figure 8-(b) the total resultant of the normal stress is shown according to Eq. 19, and compared with the 3D solid analysis obtained with ANSYS, shown in Figure 8-(a). In Figure 9, the stress τ_{xz} component is compared.

(a)σ_z stress component by warping (N/m^2) (b) σ_z stress component by bending (N/m^2)

Figure 7. Relevance of the bimoment on the normal stresses.

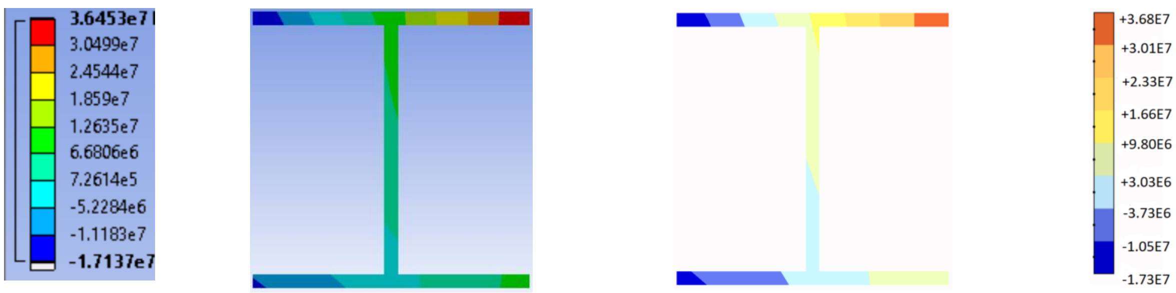

(a) σ_z stress component by ANSYS (N/m^2) (b) σ_z stress component by present study (N/m^2)

Figure 8. Comparison of the normal stress result with the response obtained with 3D solid analysis.

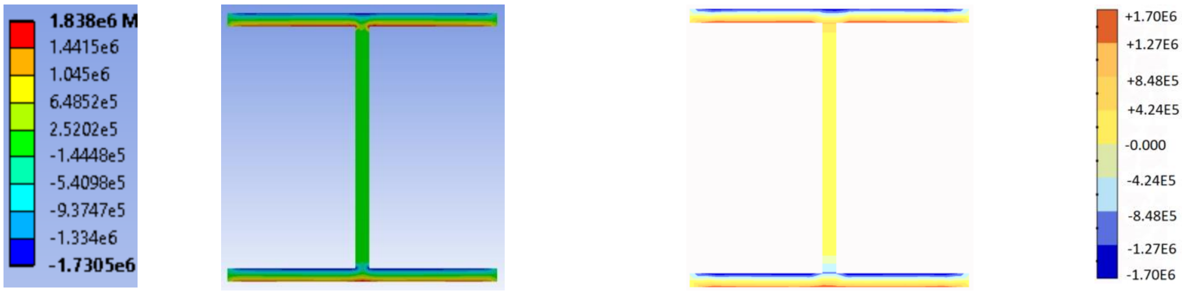

(a). τ_{xz} stress component by ANSYS (N/m2) (b) τ_{xz} stress component by present study (N/m^2)

Figure 9. Comparison of the stress component τ_{xz} with the response obtained with 3D solid analysis.

4 Conclusions

In Figure 7, it is possible to observe that the bimoment generates stresses around 30% of the stresses obtained by means of the classical beam theory, that is, it represents a very significant portion of the total normal streses and should be considered in the design of thin-walled structural elements. The good agreement of the results obtained with the present formulation with the results provided by the accurate 3D solid ANSYS models demonstrate the accuracy of the proposed formulation.

Acknowledgements. The authors thank the Graduate Program in Civil Engineering of the Federal University of Ouro Preto (PROPEC/UFOP), and the CAPES and CNPq for sponsoring this work. In addition, the first author would like to especially thank to the University of the State of Mato Grosso for supporting him during his doctoral course at PROPEC/UFOP.

References

[1] E.J. Sapountzakis and V.G. Mokos, "Secundary torsional moment deformation effect by BEM". International Journal of Mechanical Sciences 53(2011) 897-909.
[2] E.J. Sapountzakis. "Solution of non-uniform torsion of bars by an integral equation method". *Computer and Structure*s 77(2000) 659-667.
[3]de Araújo F.C. et al. Nonuniform torsion analysis in tarped composite bars by including higher-order warping modes, vol. 69, Computational Mechanics, p. 911-930.